# Conformationally Tuned Large Two-Photon Absorption Cross Sections in Simple Molecular Chromophores

**Swapan K. Pati, Tobin J. Marks,* and Mark A. Ratner***

*Contribution from the Department of Chemistry and the Materials Research Center, Northwestern University, 2145 Sheridan Road, Evanston, Illinois 60208-3113*

*Received September 11, 2000. Revised Manuscript Received March 22, 2001*

**Abstract:** We investigate here the relationship between molecular architecture and two-photon absorption (TPA) processes in a class of alkyl-substituted 4-quinopyran chromophores. We find that TPA cross sections diverge as the one-photon gap energy nears one-half of the two-photon gap. The molecular strategy proposed here to tune these two-excitation gaps for maximizing TPA cross sections is to twist the molecule about the bond connecting the chromophore donor and acceptor phenylene fragments. Extremely large TPA cross sections, determined by the absorption bandwidth, can then be realized (imaginary part of the third-order polarizability $\sim 2.6 \times 10^5 \times 10^{-36}$ esu) for fundamental photon energies near 1.0 eV, when the torsional angle approaches 104°. The required torsional angle is achieved by introduction of sterically encumbered 2,2′,2″,2‴ tertiary alkyl substituents.

## Introduction

The two-photon absorption (TPA) process was one of the first nonlinear processes to be observed experimentally, shortly after the advent of lasers.[1] More recently, improvements in experimental techniques and emerging applications have stimulated growing interest in molecular TPA processes.[2]

TPA is a nonlinear absorption process wherein two photons are absorbed simultaneously. Characteristic features are adherence to even-parity selection rules and quadratic intensity dependence, while one-photon absorption processes typically conform to odd-parity selection rules and linear intensity dependence. Molecules with large two-photon cross sections are of interest in applications as diverse as 3D optical data storage,[3] optical limiting,[4] and fluorescence microscopy.[5] These applications are primarily based on accessing higher-energy excited states using relatively low-energy laser sources, and these applications would benefit considerably from new design strategies for enhancing molecular/macromolecular TPA cross sections. We report here one such promising strategy.

When a material is subjected to an electromagnetic incident field, it is standard to develop a power series expansion of the polarization $P$, as a function of the applied electric field $\vec{E} = (E_x,E_y,E_z)$.

$$P_i(E) = \sum_j \chi_{ij}^{(1)} E_j + \frac{1}{2}\sum_{jk} \chi_{ijk}^{(2)} E_j E_k + \frac{1}{6}\sum_{jkl} \chi_{ijkl}^{(3)} E_j E_k E_l + \ldots \quad (1)$$

Here $\chi^{(n)}$ is the $n$th-order susceptibility tensor of the medium, and a schematic notation is used. Near a resonance, the susceptibility tensor becomes complex, and the imaginary part describes absorption (or gain) properties. The two-photon absorption coefficient, $\alpha_2$, is proportional to the imaginary part of the third-order susceptibility tensor.[6] At the molecular level, the macroscopic $\chi^{(3)}$ can be replaced by the third-order molecular nonlinearity. Thus, the molecular two-photon absorption cross section can be characterized by the imaginary part of the molecular third-order nonlinear polarizability, defined at an absorption frequency of $\omega$ as in eq 2[2]

$$\alpha^{(2)}(\omega) \propto \mathrm{Im}\gamma(-\omega) \quad (2)$$

where $\gamma(-\omega) = [\gamma(-\omega;\omega,\omega,-\omega)]$. The sum-over-states (SOS) expression for the third-order hyperpolarizability can be obtained from the fourth-order perturbation theory to describe the effects of an applied electric field on the molecular energy levels. It can be written as in eq 3

$$\gamma(-\omega;\omega,\omega,-\omega) = \sum_{\mathrm{BAB'}} \frac{\langle \mathrm{G}|\mu|\mathrm{B}\rangle\langle \mathrm{B}|\mu|\mathrm{A}\rangle\langle \mathrm{A}|\mu|\mathrm{B'}\rangle\langle \mathrm{B'}|\mu|\mathrm{G}\rangle}{E_{\mathrm{GB}}E_{\mathrm{GA}}E_{\mathrm{GB'}}} - \sum_{\mathrm{BB'}} \frac{\langle \mathrm{G}|\mu|\mathrm{B}\rangle\langle \mathrm{B}|\mu|\mathrm{G}\rangle\langle \mathrm{G}|\mu|\mathrm{B'}\rangle\langle \mathrm{B'}|\mu|\mathrm{G}\rangle}{E^2_{\mathrm{GB}}E_{\mathrm{GB'}}} \quad (3)$$

where |G> is the ground state and |B>, |A>, and |B′> are the excited electronic states. $\mu$ is the electric dipole operator and $E_{Gi}$ is the energy of the $i$th state relative to the ground state. The first term in the summation can be viewed as a sum over

* Corresponding author.

(1) Kauser, W.; Garrett, C. G. B. *Phys. Rev. Lett.* **1961**, *7*, 229.
(2) Kershaw, S. in *Characterization Techniques and Tabulations for Organic Nonlinear Optical Materials;* Kuzyk, M. G., Dirk, C. W., Eds.; Marcel Dekker Inc.: New York, 1998; p 515.
(3) (a) Strickler, J. H.; Webb, W. W. *Opt. Lett.* **1991**, *16*, 1780. (b) Rentzepis, P. M.; Parthenopoulos *Science* **1989**, *245*, 843.
(4) (a) Said, A. A.; Wamsely, C.; Hagan, D. J.; Van Stryland, E. W.; Reinhardt, B. A.; Rodered, P.; Dillard, A. G. *Chem. Phys. Lett.* **1994**, *228*, 646. (b) He, G. S.; Xu, G. C.; Prasad, P. N.; Reinhardt, B. A.; Bhatt, J. C.; Dillard, A. G. *Opt. Lett.* **1995**, *20*, 435. (c) Ehrlich, J. E.; Wu, X. L.; Lee, I.-Y. S.; Hu, Z.-H.; Rockel, H.; Marder, S. R.; Perry, J. W. *Opt. Lett.* **1997**, *22*, 1843.
(5) (a) Denk, W.; Striker, J. H.; Webb, W. W. *Science* **1990**, *248*, 73. (b) Kohler, R. H.; Cao, J.; Zipfel, W. R.; Webb, W. W. *Science* **1997**, *276*, 2039.
(6) (a) Prasad, P. N.; Williams, D. J. *Introduction to Nonlinear Optical Effects in Molecules and Polymers*; Wiley: New York, 1991. (b) Prasad, P. N.; Karna, S. P. *Int. J. Quantum. Chem.* **1994**, *28*, 395.

10.1021/ja0033281 CCC: $20.00 © 2001 American Chemical Society
Published on Web 07/06/2001

all possible virtual absorption processes where the transition dipoles are nonzero. However, the second term restricts the process only to the virtual one-electron excited states. Schematically, the above equation can be represented as follows: $|G\rangle \rightarrow |B\rangle \rightarrow |A\rangle \rightarrow |B'\rangle \rightarrow |G\rangle - |G\rangle \rightarrow |B\rangle \rightarrow |G\rangle \rightarrow |B'\rangle \rightarrow |G\rangle$. Thus, to obtain finite $\gamma$, states B and B′ should have finite transition dipole moments from the ground state, while the state A can have zero transition dipole from the ground state but finite from either state B or B′. By definition, the B and B′ states are called one-photon states, while the A states are called two-photon states.

Many theoretical studies have established that the dominant contributions to third-order nonlinear optical (NLO) properties come from three important terms.[7] Two of these (commonly referred to as N or negative and D or dipolar terms) involve the ground state and the lowest optically allowed one-photon state, and a third term (referred to as the T or two-photon term) involves three low-lying states, namely, the ground (G), the lowest optically allowed one-photon state (B), and an optically forbidden two-photon state (A). Explicitly, at a frequency $\omega$, these terms can be written as in eq 4:

$$\gamma_N = -P\sum_B\left[\frac{\mu_{GB}^4}{(E_{GB}-\omega-i\tau_{GB})^2(E_{GB}+\omega+i\tau_{GB})}\right] \quad (4a)$$

$$\gamma_D = P\sum_B\left[\frac{\mu_{GB}^2\Delta\mu_{GB}^2}{(E_{GB}-\omega-i\tau_{GB})^2(E_{GB}-2\omega-i\tau_{GB})}\right] \quad (4b)$$

$$\gamma_T = P\sum_{BA}\left[\frac{\mu_{GB}^2\mu_{BA}^2}{(E_{GB}-\omega-i\tau_{GB})^2(E_{GA}-2\omega-i\tau_{GA})}\right] \quad (4c)$$

where P corresponds to the permutation operator over the optical frequencies, $\mu_{ij}$ and $\Delta\mu_{ij}$ are the transition dipole moment and difference in dipole moments between states *i* and *j*, respectively. $\tau_{ij}$ corresponds to the line width of the *j*th state relative to the *i*th state.

Because the net dipole moment is zero for centrosymmetric systems, the dipolar term is present only for the noncentrosymmetric systems. The negative term contributes only at the one-photon resonance, and so it makes no important contribution to the two-photon processes. The two-photon term is the dominant term. A number of semiempirical calculations on the third-order NLO properties have demonstrated the importance of the two-photon term in determining the final value of the third-order property.[8] At a two-photon resonance condition, the two-photon term can be expressed as in eq 5[9]

$$\gamma_T \propto \frac{\mu_{GB}^2\mu_{BA}^2}{\tau(2E_{GB}-E_{GA}-2i\tau)^2} \quad (5)$$

where at the TPA resonance, $E_{GA} = 2\omega$. We have assumed here that $\tau = \tau_{GB} = \tau_{GA}$.

There are four different parameters, two excitation energies, and two transition dipole moments in the above equation, which can be tuned to obtain high TPA cross sections. According to the above equation, the energy gaps should be small, and the transition moments should be maximized to obtain reasonably high TPA cross sections. However, a unique situation can be realized if it is possible to simultaneously tune the one-photon and two-photon gaps so that the one-photon and two-photon absorptions occur at the same frequency. The prerequisite for such a regime is that the one-photon gap should be half the two-photon gap ($E_{GA} = 2E_{GB}$) and that the transition moments should be finite. This situation ensures that the TPA cross section can be tuned to a maximum. Furthermore, according to the expression for the negative term, $\gamma_N$ (eq 4a), this special crossing resonance situation should also contribute, since in this case, both one-photon and two-photon absorption occur at the same frequency. In the present contribution, we investigate those molecular stereoelectronic characteristics which may allow realization of maximum TPA responses.

## Results and Discussion

Donor−acceptor molecules constitute an important class of NLO chromophores, the response properties of which are reasonably well-characterized.[10,11] Key properties include low-lying one-photon absorptions in the visible or near IR, arising from intramolecular donor to acceptor substituent charge transfer (CT). Very large nonresonant first-order hyperpolarizabilities can originate from this CT excitation.[8a,12] To realize the above requirements for the optimized relationship of one-photon and two-photon gaps, we choose the family of donor−acceptor chromophores **I**, which can exist as a function of $\theta$, in either neutral or zwitterionic forms.

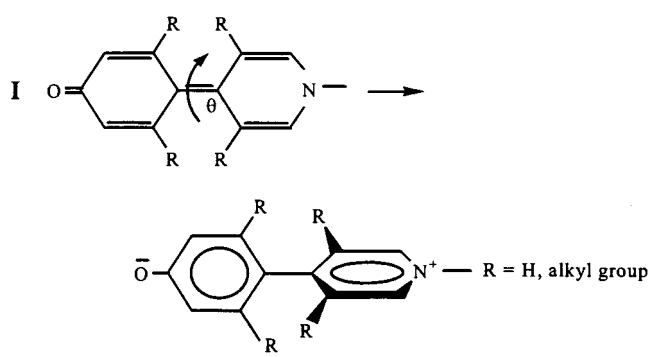


The neutral molecular structure with a quinoid geometry is the molecular ground state, while the zwitterionic configuration with a benzenoid structure contributes significantly when $\theta \neq 0$. Furthermore, this excited state is ionic and possesses a large dipole moment. The characteristic that tunes the excitation spectrum is an R-dependent steric modulation of the $\pi$-electron conjugation pathway, which for increasing $\theta$ (increasingly encumbered R substituents) enhances intramolecular CT and stabilizes the zwitterionic structure. Note that the bond connecting the donor and acceptor phenylene fragments is a double

(7) (a) Armstrong, J. A.; Bloembergen, N.; Ducuing, J.; Pershan, P. S. *Phys. Rev.* **1962**, *127*, 1918. (b) Orr, B. J.; Ward, J. F. *Mol. Phys.* **1971**, *20*, 513.

(8) (a) Albert, I. L.; Marks, T. J.; Ratner, M. A. In *Nonlinear Optical Materials: Theory and Modelling;* Karna, S. P., Yeates, A. T. Eds.; ACS Symposium Series 628; American Chemical Society: Washington, DC, 1996; p 116. (b) Meyers, F.; Marder, S. R.; Pierce, B. M.; Bredas, J. L. *J. Am. Chem. Soc.* **1994**, *116*, 10703.

(9) TPA response can be calculated from energies and transition dipole couplings. Boyd, R. W. *Nonlinear Optics*; Academic Press: London, 1992.

(10) (a) Wolff, J. J.; Wortmann, R. *Adv. Chem. Phys.* **1999,** *32*, 121. (b) Kuzyk, M. G. *Phys. Rev. Lett.* **2000**, *85*, 1218.

(11) Large optical nonlinearities and sub-psec response times are also observed in conjugated polymers. (a) Chemla, D. S., Zyss, J., Eds. *Nonlinear Optical Properties of Organic Molecules and Crystals*; Academic Press: Orlando, 1987. (b) Messier, J., Ed. *Nonlinear Optical Effects in Organic Polymers*; Kluwer: Boston, 1988.

(12) (a) Albert, I. D. L.; Marks, T. J.; Ratner, M. A. *J. Am. Chem. Soc.* **1998**, *120*, 11174. (b) Albert, I. D. L.; Marks, T. J.; Ratner, M. A. *J. Am. Chem. Soc.* **1997,** *109*, 3155.

**Table 1.** Interatomic Distances (in Å) and Angles (in Degrees) for Optimized Structure **I** with R = H

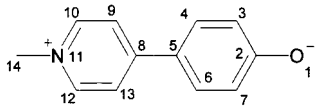


| Interatomic Deistances | | | |
|---|---|---|---|
| bond | length | bond | length |
| C2−O1 | 1.243 | C3−C2 | 1.467 |
| C4−C3 | 1.348 | C5−C4 | 1.449 |
| C6−C5 | 1.449 | C7−C2 | 1.467 |
| C7−C6 | 1.348 | C8−C5 | 1.379 |
| C9−C8 | 1.447 | C10−C9 | 1.367 |
| N11−C10 | 1.385 | C12−N11 | 1.386 |
| C13−C8 | 1.447 | C13−C12 | 1.366 |
| C14−N11 | 1.437 | H15−C7 | 1.101 |
| H16−C6 | 1.101 | H17−C4 | 1.101 |
| H18−C3 | 1.101 | H19−C13 | 1.099 |
| H20−C12 | 1.105 | H21−C10 | 1.105 |
| H22−C9 | 1.099 | H23−C14 | 1.122 |
| H24−C14 | 1.124 | H25−C14 | 1.124 |

| Bond Angles | | | | | |
|---|---|---|---|---|---|
| angle | degrees | angle | degrees | angle | degrees |
| O1−C2−C3 | 122.49 | O1−C2−C7 | 122.48 | C3−C2−C7 | 115.03 |
| C2−C3−C4 | 121.95 | C2−C3−H18 | 116.29 | C4−C3−H18 | 121.76 |
| C3−C4−C5 | 122.85 | C3−C4−H17 | 118.87 | C5−C4−H17 | 118.28 |
| C4−C5−C6 | 115.38 | C4−C5−C8 | 122.31 | C6−C5−C8 | 122.30 |
| C5−C6−C7 | 122.85 | C5−C6−H16 | 118.28 | C7−C6−H16 | 118.88 |
| C2−C7−C6 | 121.95 | C2−C7−H15 | 116.30 | C6−C7−H15 | 121.75 |
| C5−C8−C9 | 123.03 | C5−C8−C13 | 123.00 | C9−C8−C13 | 113.97 |
| C8−C9−C10 | 121.94 | C8−C9−H22 | 119.87 | C10−C9−H22 | 118.19 |
| C9−C10−N11 | 122.16 | C9−C10−H21 | 121.87 | N11−C10−H21 | 115.97 |
| C10−N11−C12 | 117.85 | C10−N11−C14 | 121.83 | C12−N11−C14 | 120.32 |
| N11−C12−C13 | 122.22 | N11−C12−H20 | 115.61 | C13−C12−H20 | 122.17 |
| C8−C13−C12 | 121.86 | C8−C13−H19 | 119.88 | C12−C13−H19 | 118.25 |
| N11−C14−H23 | 110.24 | N11−C14−H24 | 109.90 | N11−C14−H25 | 109.95 |
| H23−C14−H24 | 108.94 | H23−C14−H25 | 108.95 | H24−C14−H25 | 108.83 |

bond when the molecule is neutral, while it is single bond for the zwitterionic structure. To investigate $\theta$-dependent effects on the excitation spectrum, the geometry was optimized using the AM1 parametrized Hamiltonian. The optimized R = H structure is found to be planar with electronic delocalization over the entire molecule. The derived molecular metrical parameters are compiled in Table 1. $\theta$ was then varied without geometry optimizing the twisted structures.[12] As we incrementally increase $\theta$, the bond-order calculations show that the twisted double bond slowly transforms into a single bond. Also, the nitrogen and oxygen atoms accumulate positive and negative charge, respectively, as $\theta$ is increased, thus confirming qualitative valence bond expectations about the consequences of twisting.

Computations of two-photon absorptions used Zerner's INDO method,[13] with the levels of CI calculation varied—singles/doubles (SDCI), singles/doubles with pair excitations (PECI), multireference doubles CI (MRDCI)—to reliably estimate the third-order response. The PECI and MRDCI results are comparable, and MRDCI results with four reference determinants are reported. For each reference, we utilized five-occupied and five-unoccupied MOs to construct a CI space with a configuration dimension of 600−700. The sum-over-states method was then used to calculate TPA coefficients. In all calculations, a constant damping factor of $\tau = 0.1$ eV was employed.[14]

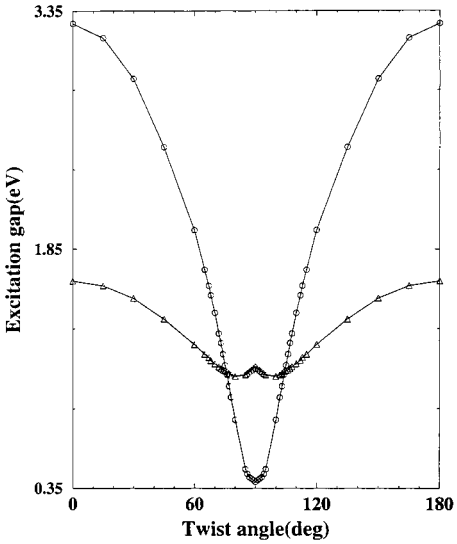


**Figure 1.** One-photon excitation gap (circles) and one-half of the two-photon excitation gap (triangles) as a function of twist angle $\theta$ in chromophore **I**. Energies are in eV units.

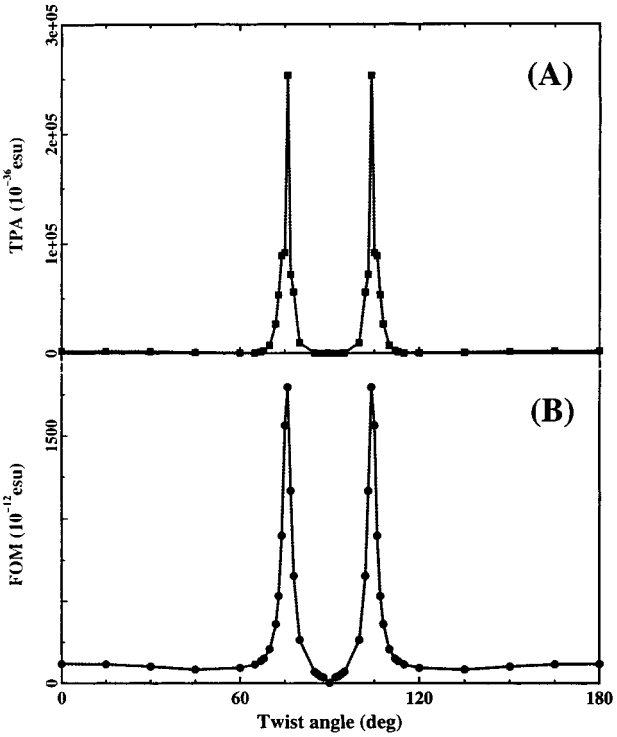


**Figure 2.** A. Variation of the imaginary part of the third-order polarizability in units of $10^{-36}$ esu. B. The chromophore figure of merit (FOM) in units of $10^{-12}$ esu, with the twist angle $\theta$ in chromophore **I**. These values are computed at the resonant TPA frequencies for the corresponding $\theta$.

In Figure 1, the computed variation of the one-photon gap and one-half the two-photon gap in chromophore **I** with $\theta$ are shown. The one-photon gap exhibits a single-well structure with a minimum at $\theta = 90°$. However, the two-photon gap, which is almost degenerate with the one-photon gap in the planar structure, exhibits a double-well pattern. Most importantly, at two symmetrically disposed $\theta$ values close to the minima, the one-half two-photon gaps become nearly equal to the one-photon gap, which should result in very large TPA cross sections. Note

(13) (a) Ridley, J.; Zerner, M. C. *Theor. Chim. Acta* **1973,** *32,* 111. (b) Bacon, A. D.; Zerner, M. C. *Theor. Chim. Acta* **1979**, *53,* 21.

(14) Assuming a constant dephasing time of the electronic excitations for each structure is a pragmatic approximation. For a more quantitative study, it would be necessary to use proper damping factors for each particular structure since the TPA intensity $\sim\tau^{-1}$ (or at the maxima in Figure 2, $\sim\tau^{-3}$). Stegeman, G. I.; Torruellas, W. E. *Philos. Trans. R. Soc. London, Ser. A* **1996,** *354,* 745.

**Table 2.** Interatomic Distances (in Å) and Bond Angles (in Degrees) for Optimized Structure **I** with R = *tert*-Butyl

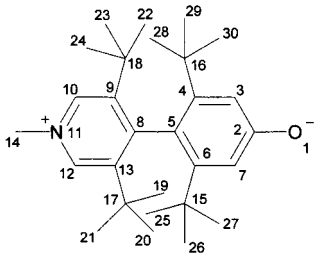


Interatomic Distances

| bond | length | bond | length | bond | length |
|---|---|---|---|---|---|
| C2−O1 | 1.256 | C3−C2 | 1.445 | C4−C3 | 1.373 |
| C5−C4 | 1.445 | C6−C5 | 1.437 | C7−C2 | 1.440 |
| C7−C6 | 1.376 | C8−C5 | 1.446 | C9−C8 | 1.441 |
| C10−C9 | 1.401 | N11−C10 | 1.365 | C12−N11 | 1.367 |
| C13−C8 | 1.442 | C13−C12 | 1.400 | C14−N11 | 1.448 |
| H15−C7 | 1.100 | C16−C6 | 1.528 | C17−C4 | 1.528 |
| H18−C3 | 1.100 | C19−C13 | 1.524 | H20−C12 | 1.108 |
| H21−C10 | 1.108 | C22−C9 | 1.524 | H23−C14 | 1.122 |
| H24−C14 | 1.123 | H25−C14 | 1.123 | C26−C19 | 1.520 |
| C27−C19 | 1.533 | C28−C19 | 1.536 | C29−C22 | 1.520 |
| C30−C22 | 1.535 | C31−C22 | 1.535 | C32−C16 | 1.520 |
| C33−C16 | 1.533 | C34−C16 | 1.535 | C35−C17 | 1.536 |
| C36−C17 | 1.524 | C37−C17 | 1.523 | H38−C26 | 1.118 |
| H39−C26 | 1.115 | H40−C26 | 1.116 | H41−C27 | 1.115 |
| H42−C27 | 1.118 | H43−C27 | 1.116 | H44−C28 | 1.114 |
| H45−C28 | 1.118 | H46−C28 | 1.116 | H47−C29 | 1.118 |
| H48−C29 | 1.116 | H49−C29 | 1.115 | H50−C30 | 1.117 |
| H51−C30 | 1.118 | H52−C30 | 1.114 | H53−C31 | 1.116 |
| H54−C31 | 1.118 | H55−C31 | 1.116 | H56−C32 | 1.120 |
| H57−C32 | 1.114 | H58−C32 | 1.114 | H59−C33 | 1.115 |
| H60−C33 | 1.118 | H61−C33 | 1.115 | H62−C34 | 1.115 |
| H63−C34 | 1.118 | H64−C34 | 1.115 | H65−C35 | 1.118 |
| H66−C35 | 1.116 | H67−C35 | 1.116 | H68−C36 | 1.114 |
| H69−C36 | 1.118 | H70−C36 | 1.116 | H71−C37 | 1.115 |
| H72−C37 | 1.119 | H73−C37 | 1.114 | | |

Bond Angles

| angle | degrees | angle | degrees | angle | degrees |
|---|---|---|---|---|---|
| O1−C2−C3 | 122.37 | O1−C2−C7 | 122.74 | C3−C2−C7 | 114.89 |
| C2−C3−C4 | 123.94 | C2−C3−H18 | 112.51 | C4−C3−H18 | 123.54 |
| C3−C4−C5 | 118.98 | C3−C4−C17 | 115.40 | C5−C4−C17 | 125.52 |
| C4−C5−C6 | 119.08 | C4−C5−C8 | 121.02 | C6−C5−C8 | 119.89 |
| C5−C6−C7 | 119.74 | C5−C6−C16 | 127.60 | C7−C6−C16 | 112.55 |
| C2−C7−C6 | 123.37 | C2−C7−H15 | 114.82 | C6−C7−H15 | 121.80 |
| C5−C8−C9 | 121.13 | C5−C8−C13 | 121.65 | C9−C8−C13 | 117.21 |
| C8−C9−C10 | 119.14 | C8−C9−C22 | 128.64 | C10−C9−C22 | 112.06 |
| C9−C10−N11 | 122.76 | C9−C10−H21 | 121.52 | N11−C10−H22 | 115.71 |
| C10−N11−C12 | 118.70 | C10−N11−C14 | 121.36 | C12−N11−C14 | 119.93 |
| N11−C12−C13 | 123.02 | N11−C12−H20 | 115.19 | C13−C12−H20 | 121.78 |
| C8−C13−C12 | 118.88 | C8−C13−C19 | 129.03 | C12−C13−C19 | 112.07 |
| N11−C14−H23 | 110.22 | N11−C14−H24 | 109.45 | N11−C14−H25 | 109.47 |
| H23−C14−H24 | 109.14 | H23−C14−H25 | 109.22 | H24−C14−H25 | 109.32 |
| C6−C16−C32 | 117.79 | C6−C16−C33 | 109.71 | C6−C16−C34 | 108.80 |
| C32−C16−C33 | 106.55 | C32−C16−C34 | 106.16 | C33−C16−C34 | 107.35 |
| C4−C17−C35 | 112.55 | C4−C17−C36 | 112.15 | C4−C17−C37 | 113.34 |
| C35−C17−C36 | 105.26 | C35−C17−C37 | 105.29 | C36−C17−C37 | 107.67 |
| C13−C19−C26 | 115.57 | C13−C19−C27 | 109.67 | C13−C19−C28 | 109.68 |
| C26−C19−C27 | 107.64 | C26−C19−C28 | 107.13 | C27−C19−C28 | 106.77 |
| C9−C22−C29 | 115.83 | C9−C22−C30 | 110.42 | C9−C22−C31 | 108.63 |
| C29−C22−C30 | 117.64 | C29−C22−C31 | 107.15 | C30−C22−C31 | 106.76 |
| C19−C26−H38 | 109.20 | C19−C26−H39 | 111.24 | C19−C26−H40 | 111.29 |
| H38−C26−H39 | 108.92 | H38−C26−H40 | 108.14 | H39−C26−H40 | 107.96 |
| C19−C27−H41 | 111.63 | C19−C27−H42 | 109.18 | C19−C27−H43 | 111.10 |
| H41−C27−H42 | 108.39 | H41−C27−H43 | 108.76 | H42−C27−H43 | 107.67 |
| C19−C28−H44 | 111.61 | C19−C28−H45 | 111.22 | C19−C28−H46 | 111.65 |
| H44−C28−H45 | 107.94 | H44−C28−H46 | 108.91 | H45−C28−H46 | 107.35 |
| C22−C29−H47 | 109.13 | C22−C29−H48 | 111.24 | C22−C29−H49 | 111.42 |
| H47−C29−H48 | 108.21 | H47−C29−H49 | 108.81 | H48−C29−H49 | 107.96 |
| C22−C30−H50 | 111.41 | C22−C30−H51 | 109.36 | C22−C30−H52 | 111.89 |
| H50−C30−H51 | 107.30 | H50−C30−H52 | 108.74 | H51−C30−H52 | 107.96 |
| C22−C31−H53 | 110.98 | C22−C31−H54 | 109.12 | C22−C31−H55 | 111.55 |
| H53−C31−H54 | 107.78 | H53−C31−H55 | 108.87 | H54−C31−H55 | 108.44 |
| C16−C32−H56 | 109.36 | C16−C32−H57 | 111.41 | C16−C32−H58 | 111.52 |
| H56−C32−H57 | 107.68 | H56−C32−H58 | 107.56 | H57−C32−H58 | 109.22 |
| C16−C33−H59 | 111.27 | C16−C33−H60 | 109.64 | C16−C33−H61 | 111.05 |
| H59−C33−H60 | 108.26 | H59−C33−H61 | 108.29 | H60−C33−H61 | 108.23 |
| C16−C34−H62 | 110.80 | C16−C34−H63 | 109.77 | C16−C34−H64 | 111.23 |
| H62−C34−H63 | 108.36 | H62−C34−H64 | 108.36 | H63−C34−H64 | 108.24 |
| C17−C35−H65 | 109.42 | C17−C35−H66 | 110.86 | C17−C35−H67 | 110.87 |
| H65−C35−H66 | 107.90 | H65−C35−H67 | 107.92 | H66−C35−H67 | 109.77 |
| C17−C36−H68 | 110.20 | C17−C36−H69 | 110.01 | C17−C36−H70 | 110.73 |
| H68−C36−H69 | 107.84 | H68−C36−H70 | 109.88 | H69−C36−H70 | 108.10 |
| C17−C37−H71 | 110.97 | C17−C37−H72 | 109.96 | C17−C37−H73 | 110.21 |
| H71−C37−H72 | 107.97 | H71−C37−H73 | 110.01 | H72−C37−H73 | 107.64 |

that the two-photon absorption frequency (half the two-photon gap) at these minima is ∼1.0 eV, which is rather small compared to those values found in molecular chromophores examined previously.[15]

The above variation in one-photon and two-photon states with $\theta$ can be understood as follows.

In the planar geometry ($\theta = 0°$), the excitations include contributions from both quinoid and aromatic structures. However, progressing to $\theta \neq 0°$ reduces the delocalization between donor and acceptor fragments by a factor proportional to cos $\theta$. As $\theta$ increases, the mixing decreases, and simultaneously, the CT excitation oscillator strength diminishes. Thus, the effect of the twist is to progressively enforce electron localization and, consequently, the excitations correspond to progressively more local excitations. Additionally, analysis of the CI basis reveals that at small $\theta$, the B state consists of (i) one-electron HOMO → LUMO excitation and (ii) a HOMO → (LUMO+1) pair excitation, while for the A state, the excitations consist of (i) a single excitation involving HOMO and (LUMO+1) and (ii) a double excitation involving HOMO, LUMO, and (LUMO+1). As $\theta$ increases, the weight of excitation (ii) in both cases decreases, and near $\theta \sim 75°$ and $\theta \sim 85°$ for the A and B states, respectively, the excitations are predominantly type (i) for each case, that is, resembling a single-electron picture. Correspondingly, the B state oscillator strength falls with an increase in $\theta$, suggesting that the B state, which is a bound-electron-hole state (exciton state) at small $\theta$ values, slowly transforms to a free-one-electron excited state with increasing $\theta$.

In Figure 2A, the imaginary part of $\gamma(-\omega;\omega,\omega,-\omega)$,which is a tumbling average response function computed as in eq 6, is plotted as a function of $\theta$.

$$\gamma = \frac{1}{15}\sum_{i,j=x,y,z}(2\gamma_{iijj} + \gamma_{ijji}) \qquad (6)$$

As expected, the TPA cross section diverges at the two values of $\theta$ where one-half of the two-photon energies equals the one-photon energies. The $\theta$ values for TPA maxima are at 76° and 104°—symmetric around the perpendicular conformation. The realistic molecular means of enforcing the change in dihedral angles involves introducing various alkyl groups at the R positions in structure **I**. The substituted chromophores were fully optimized using the AM1 Hamiltonian. The fully optimized structure with four *t*-Bu groups at the 2,2′,2″,2‴ positions gives the required twist angle of 104°. Computed molecular metrical parameters are compiled in Table 2. The calculated imaginary part of $\gamma(-\omega;\omega,\omega,-\omega)$ for this chromophore is found to be very large, $\sim 2 \times 10^5 \times 10^{-36}$ esu. Remarkably, the response is several orders of magnitude larger than any molecular TPA parameters reported to date.[15,16]

The performance of any NLO material is indexed by a figure of merit (FOM). Here it is defined as[17] $\gamma(-\omega;\omega,\omega,-\omega)/\alpha(\omega)$, where $\alpha(\omega)$ is the linear absorption coefficient. According to

(15) (a) Marder, S. R.; Gorman, C. B.; Meyers, F.; Perry, J. W.; Bourhill, G.; Bredas, J. L.; Pierce, B. M. *Science* **1994**, *265*, 632. (b) Kogej, T.; Beljonne, D.; Perry, J. W.; Marder, S. R.; Bredas, J. L. *Chem. Phys. Lett.* **1998**, *298*, 1. (c) Albota, M.; et al. *Science* **1998**, *281*, 1653.

(16) The present responses compare favorably with those of very high response conjugated polymeric systems: (a) Lawrence, B.; Torruellas, W. E.; Cha, M.; Sundheimer, M. L.; Stegeman, G. I.; Meth, J.; Etemad, S.; Bake, G. *Phys. Rev. Lett.* **1994**, *73*, 597. (b) Mathy, A.; Ueberhofen, K.; Schenk, R.; Gregorius, H.; Garay, R.; Mullen, K.; Bubeck, C. *Phys. Rev. B.* **1996**, *53*, 4367.

(17) Stegeman, G. I.; Torruellas, W. E. *Philos. Trans. R. Soc. London, Ser. A* **1996**, *354*, 745.

eq 3, the crossing points of Figure 1 correspond to triply degenerate situations, and at those critical $\theta$ values, $\gamma \sim \text{const}/\tau^3$ and $\alpha \sim \text{const}/\tau$, and so FOM $\sim \text{const}/\tau^2$. This suggests that the imaginary part of the spectral density component will actually determine both $\gamma$ and $\alpha$, exactly at or very near the critical $\theta$. Such behavior is standard for Lorentzian lines. The important point is simply that the special crossing (Figure 1) will yield very large $\gamma$ and FOM values for a given $\tau$, compared to any system without the crossing resonance (for which $\gamma$ at resonance $\sim \text{const}/\tau(E - \omega)^2$ ). We plot FOM as a function of $\theta$ in Figure 2B. These values are significantly larger than those reported to date for typical conjugated polymers ($\sim 5 \times 10^{-14}$ esu cm).[16,18]

In summary, the present computational results offer a new design strategy to enhance molecular TPA cross sections, and in turn, new strategies for molecule-based photonic materials as varied as tunable laser materials and chromophores for biological fluorescence microscopy.[19] Furthermore, the sub-psec response of organic systems having very large TPA parameters may prove advantageous in all-optical switching for high speed optical networks.[20]

**Acknowledgment.** We thank Dr. I. D. L. Albert for substantiative advice in this research. We are grateful to the MRSEC program of NSF for support of this research through the Northwestern Materials Research Center (Grant DMR-0076097).

JA0033281

(18) Buheck, C.; Kaltbeitzel, A.; Grund, A.; Leclerc, M. *Chem. Phys.* **1991**, *154*, 343.

(19) Xu, C.; Webb, W. W. *J. Opt. Soc. Am. B* **1996**, *13*, 481.

(20) (a) Nakamura, S.; Ueno, Y.; Tajima, K. *IEEE Photon. Tech. Lett.* **1998**, *10*, 1575. (b) Stegeman, G. I.; Miller, A. In *Photonics Switching*; Midwinter, J. E., Ed.; Academic Press: San Diego, CA, 1993; Vol. 1, Chapter 5.